THE JOURNAL OF PHYSICAL CHEMISTRY C

Article

pubs.acs.org/JPCC

Lithium Borohydride Ethylenediaminates: A Case Study of Solid-State $LiBH_4$–Organic Amine Complexes

Juner Chen,[†,‡] Teng He,[†] Guotao Wu,*[,†] Zhitao Xiong,[†] Lin Liu,[†] Xiaohua Ju,[†] and Ping Chen*[,†]

[†]Dalian National Laboratory for Clean Energy, Dalian Institute of Chemical Physics, Chinese Academy of Sciences, Dalian 116023, China

[‡]University of Chinese Academy of Sciences, Beijing 100049, China

Supporting Information

ABSTRACT: Nitrogen (N) containing ligands, such as ammonia (NH_3), hydrazine (N_2H_4), and ethylenediamine (en), can form a series of complexes with common features in crystal structures and thermal behaviors by coordinating with $LiBH_4$. Two newly synthesized lithium borohydride ethylenediaminates were investigated in this work. Through comparing the crystal structures of $LiBH_4$–en, $LiBH_4$–NH_3, and $LiBH_4$–N_2H_4 complexes, similar coordination environments of Li were observed in which they have the same Li/N molar ratios. Meanwhile, the establishment of dihydrogen bonding networks, together with the Li^+/N containing ligand interactions, may be important reasons for the structural stabilization and are expected to have profound impacts on their thermal behaviors. When heated under Ar flow, $LiBH_4$–N containing complexes decompose via desorption of N containing ligands followed by dehydrogenation. The coordination strength is affected by the number of ligands, i.e., with the increase of N/Li ratio the ligands can be released more easily. For dehydrogenation, the complex with the shortest NH···HB distance gave rise to the lowest initial temperature. When heated in a closed system, direct dehydrogenation can be achieved at relatively low temperatures with Co-based catalyst. About 8.5 and 7.7 wt % of hydrogen can be released from Co-catalyzed $LiBH_4$·en and $(LiBH_4)_2$·en at 180 °C, respectively.

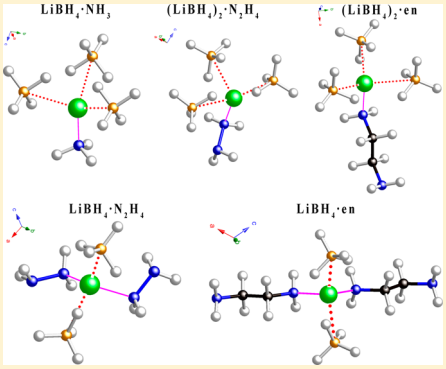

INTRODUCTION

Alkali metal borohydrides, such as $LiBH_4$, $NaBH_4$, and KBH_4, constitute an important class of reducing reagents,[1−5] starting materials for synthesis of organometallic derivatives, precursors for the production of borides and hydrides, and catalysts for hydrogenation, isomerization, oligomerization, and polymerization.[6,7] Recently, metal borohydrides have also been used as hydrogen storage materials because of their high hydrogen contents,[8−10] and $LiBH_4$ has been studied most comprehensively among the different metal borohydrides.[11] As a crystalline compound containing tetrahedral borohydride ions with an orthorhombic structure, pure $LiBH_4$ was first synthesized by the reaction of ethyllithium with diborane in 1940.[12,13] The thermogram of $LiBH_4$ shows three endothermic features: at 108−112, 258−286, and 483−492 °C.[14,15] The first feature corresponds to the reversible polymorphic transformation of $LiBH_4$. The second peak is attributed to the fusion of $LiBH_4$, which is accompanied by a slight decomposition with approximately 2% of the hydrogen evolution. The main gas desorption peak starts at 380 °C and liberates 80% of hydrogen in $LiBH_4$. Due to the high hydrogen gravimetric density (18.4 wt %) and high volumetric hydrogen density (121 kg H_2 m^{-3}), $LiBH_4$ has been widely investigated as a hydrogen storage material since 2003.[10] Additionally, $LiBH_4$ is also a starting material for the synthesis of other borohydrides through metathesis reaction with corresponding salts.[16−18] Hydrolysis reaction of $LiBH_4$ can be used for generation of H_2.[19] More recently, $LiBH_4$ has been used as a solid electrolyte in lithium batteries for its high lithium ion conductivity.[20−24]

On the other hand, $LiBH_4$ can be used to form new complexes with ligands to improve the chemical properties and augment its application. By coordination with nitrogen (N) or oxygen (O) containing ligands, a variety of $LiBH_4$-based new complexes have been synthesized (Tables S1∼S2, Supporting Information).[25−35] A fair number of these complexes have been characterized, and the structures of $LiBH_4$·nL compounds depend on the type and number (n) of ligand molecules (L).[36,37] Additionally, it is important to understand the coordination environment of the metal center because this may have an influence on the chemical behavior of a particular complex. However, only several kinds of complexes such as $LiBH_4$–NH_3,[32] $LiBH_4$–N_2H_4,[31] $LiBH_4$–NH_3BH_3,[33] $LiBH_4$–guanidine borohydride,[34] and $LiBH_4$–melamine[29] have been studied for their thermal decomposition properties. Compared with pristine $LiBH_4$, these complexes show improved dehydrogenation properties.

Organic amines are a group of chemical compounds that have a common feature of possessing sp^3-hybridized nitrogen

Received: March 29, 2014
Revised: June 11, 2014
Published: June 11, 2014

   dx.doi.org/10.1021/jp503123d | J. Phys. Chem. C 2014, 118, 13451−13459

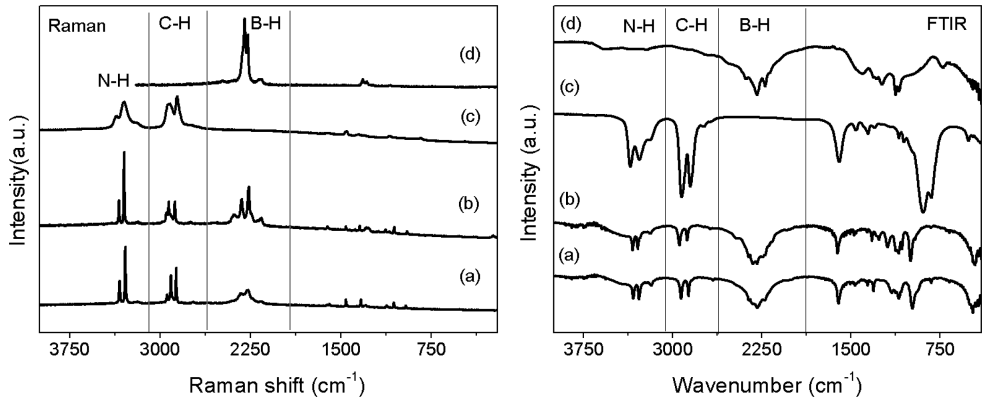

Figure 1. Raman and FTIR spectra of (a) $LiBH_4$·en, (b) $(LiBH_4)_2$·en, (c) en, and (d) $LiBH_4$.

atoms with lone pair electrons.[38] In this study, we tried to find out the common features of N-containing ligand coordinated $LiBH_4$ complexes. Thus, the simplest diamine, ethylenediamine ($NH_2CH_2CH_2NH_2$, en), was selected as a representative of organic amines to complex with $LiBH_4$. Crystal structures and thermal decomposition behaviors of $LiBH_4$ ethylenediaminates were systematically investigated in comparison with $LiBH_4$–N_2H_4 and $LiBH_4$–NH_3 complexes in this work. These newly synthesized compounds may be useful for the controlled and safe delivery of hydrogen to proton exchange membrane fuel cells (PEMFCs).[23]

EXPERIMENTAL SECTION

Synthesis. Lithium borohydride ($LiBH_4$, 95%, Acros Organics), $CoCl_2$ (97%, Sigma-Aldrich), and ethylenediamine ($NH_2CH_2CH_2NH_2$, en, 99.5% Fluka) were commercial products and used without further purification. The lithium borohydride ethylenediaminates (denoted as $(LiBH_4)_2$·en, $LiBH_4$·en, and $LiBH_4$·2en) were prepared by ball milling the solid lithium borohydride and liquid en in a Retsch PM 400 planetary mill. Composites of $(LiBH_4)_n$–en (n = 3 and 5) were prepared by the same method. Approximately 600 mg of a sample mixture was loaded into a 180 mL vessel and then milled at 200 rpm for 4 h. The ball to powder ratio was 50:1. To add Co-catalyst to the resulting borohydride ethylenediaminates, 2 mol % (per $LiBH_4$) $CoCl_2$ precursor was ball milled with $(LiBH_4)_2$·en and $LiBH_4$·en at 200 rpm for 8 h. All the sample operations were performed in an MBRAUN 200 glovebox filled with purified argon (O_2 and H_2O concentrations were below 1 ppm).

Characterization. X-ray diffraction (XRD) measurements were conducted using a PANalytical X'pert diffractometer (Cu Kα radiation, 40 kV, 40 mA). An in situ cell was used to avoid sample exposure to air during the measurement. High-resolution X-ray diffraction pattern was collected at room temperature at the BL14B1 beamline of Shanghai Synchrotron Radiation Facility (SSRF), Shanghai, China. The obtained XRD patterns have been used for indexing, simulated annealing, and refinement of the structure model using Materials Studio. [BH_4^-] and en are treated as rigid bodies. Thermogravimetric and differential thermal analysis (TG-DTA) measurements were carried out on a Netzsch TG-DTA apparatus (Netzsch, Germany). A 10 mg sample was heated in an Al_2O_3 crucible at 1 °C min^{-1} under the Ar flow. Melting point and freezing point measurements of $(LiBH_4)_2$·en and $LiBH_4$·en were performed by heating (1 °C min^{-1}) and cooling (0.2 °C min^{-1}) the samples between room temperature and 130 °C. Hydrogen desorption measurements were performed over a homemade temperature-programmed desorption (TPD) system comprising a small reactor and a mass spectrometer (MS, Hiden HPR-20) at 2 °C min^{-1} under the Ar flow. Quantitative measurements of hydrogen desorption from lithium borohydride ethylenediaminates were conducted using a Sievert-type apparatus. An ca. 200 mg sample was heated inside a closed chamber, with a heating rate of 2 °C min^{-1}. The pressure increase in the chamber was monitored, and at the heating intervals a small amount of gaseous product will be connected from the pressurized chamber to MS for analysis. Solid-state ^{11}B and ^{7}Li magic angle spinning nuclear magnetic resonance (MAS NMR) and ^{13}C cross-polarization magic angle spinning nuclear magnetic resonance (CPMAS NMR) were performed on a Bruker AVANCE 500 MHz NMR spectrometer (11.7 T). Fourier transform infrared spectroscopy (FTIR) and Raman spectra were recorded by using a Varian 3100 unit and a Renishaw inVia Raman Microscope, respectively.

RESULTS AND DISCUSSION

Complex Preparation. It is reported that NH_3 can be easily reacted with $LiBH_4$ and form ammoniates with various molar ratios, i.e., $Li(NH_3)_nBH_4$ ($0 < n \leq 4$).[30] Recently, solid-state $LiBH_4$·NH_3 and $LiBH_4$·$3NH_3$ as well as liquid $LiBH_4$·$2NH_3$ have been obtained by Guo et al. as hydrogen storage materials, but the $LiBH_4$·$2NH_3$ and $LiBH_4$·$3NH_3$ were unstable without ammonia pressure.[39] He et al. reported that reaction of hydrazine with $LiBH_4$ in various molar ratios (2/1, 1/1, 1/2, and 1/3) yields a series of new phases.[31,40]

Here, ethylenediamine ($NH_2CH_2CH_2NH_2$, en) was employed as a representative of organic amines to coordinate with $LiBH_4$ in comparison with $LiBH_4$–N_2H_4 and $LiBH_4$–NH_3 complexes. Reaction of $LiBH_4$ and en also leads to the formation of three complexes of $(LiBH_4)_2$·en, $LiBH_4$·en, and $LiBH_4$·2en. Among the three complexes is $LiBH_4$·2en, an ionic compound containing chains of cationic $[Li(en)_2]^+$ units, which has been synthesized by Giese et al.[41] We found that $LiBH_4$·2en was unstable at room temperature, and considerable en ligands could be easily detached at around 140 °C (Figure S1, Supporting Information). Therefore, we will focus on the structures and properties of $(LiBH_4)_2$·en and $LiBH_4$·en in the present work. As shown in Figure S9 (Supporting Information), white powder samples of $(LiBH_4)_2$·en and $LiBH_4$·en can be obtained by ball milling $LiBH_4$ and en. When Co-based catalyst was added, the color of the samples turned black. The samples

dx.doi.org/10.1021/jp503123d | J. Phys. Chem. C 2014, 118, 13451–13459

Table 1. Summary of Crystallographic Details for $(LiBH_4)_2$·en, $LiBH_4$·en, $(LiBH_4)_2$·N_2H_4, $LiBH_4$·N_2H_4, and $LiBH_4$·NH_3 Complexes

parameters	$(LiBH_4)_2$·en	$LiBH_4$·en	$(LiBH_4)_2$·N_2H_4	$LiBH_4$·N_2H_4	$LiBH_4$·NH_3
formula sum	$Li_8B_8C_8N_8H_{64}$	$Li_2B_2C_4N_4H_{24}$	$Li_8B_8N_8H_{48}$	$Li_8B_8N_{16}H_{64}$	$Li_4B_4N_4H_{28}$
mol. mass [g·mol^{-1}]	414.68	163.78	302.48	430.64	155.28
crystal system	monoclinic	monoclinic	orthorhombic	monoclinic	orthorhombic
space group	$P2_1/c$	Pn	$P2_12_12_1$	Cc	$Pnma$
a [Å]	17.1333(18)	8.2428(22)	7.6930(7)	12.1653(16)	5.97213(2)
b [Å]	4.5202(4)	5.2363(4)	11.9132(12)	6.7288(8)	4.46432(1)
c [Å]	11.4634(10)	8.2364(21)	6.8954(11)	10.3724(11)	14.34875(0)
α [°]	90	90	90	90	90
β [°]	106.158(5)	116.110(3)	90	104.751(5)	90
γ [°]	90	90	90	90	90
V [Å^3]	852.72	319.22	631.95(13)	821.08(17)	382.6
ρ [g cm^{-3}]	0.8078	0.8523	0.7951	0.8712	0.6748

are stable in inert atmosphere, but they are deliquescent in damp air. As shown in Figure S10 (Supporting Information), $LiBH_4$ ethylenediaminates as well as the Co-doped samples react completely with water within 5 min. Therefore, all the operations and measurements should avoid sample exposure to air.

Figure 1 shows the Raman and FTIR spectra of $(LiBH_4)_2$·en and $LiBH_4$·en including those of the pristine $LiBH_4$ and en. Raman results show that the stretching and deformation of B−H bonds in $LiBH_4$ are in the regions of 2115−2400 cm^{-1} and 1270−1350 cm^{-1}. The stretching band of B−H bonds splits into three peaks centered at 2167, 2270, and 2296 cm^{-1}, respectively, while the bending band splits into two peaks at 1288 and 1319 cm^{-1}, respectively. The N−H stretching and bending bands of en are in the regions of 3150−3420 cm^{-1} and 1560−1650 cm^{-1}. Symmetric and asymmetric N−H stretching vibrations can be easily identified at 3298 and 3365 cm^{-1}, respectively. The C−H stretching band of en is in the region of 2635−3050 cm^{-1}. All signals of B−H, N−H, and C−H vibrations are found in $LiBH_4$ ethylenediaminates. However, due to the complicated coordination environments, the vibration bands split into more peaks. For $(LiBH_4)_2$·en, B−H stretching vibrations give three contributions at 2159, 2273, and 2326 cm^{-1}; N−H stretching vibrations give two contributions at 3288 and 3335 cm^{-1}; and the stretching band of C−H bonds splits into three peaks at 2878, 2927, and 2945 cm^{-1}. For $LiBH_4$·en, however, B−H stretching vibrations are associated with five peaks at 2158, 2240, 2265, 2322, and 2387 cm^{-1}; N−H stretching vibrations are related to two sharp peaks at 3298 and 3340 cm^{-1}; and C−H stretching vibrations are found at 2866, 2909, and 2943 cm^{-1}. All B−H, N−H, and C−H vibrations in the newly synthesized complexes are close to those of pristine en and $LiBH_4$. Only slightly red shifts of B−H and N−H stretching vibrations in $LiBH_4$·en and $(LiBH_4)_2$·en, indicating the weakening of B−H and N−H bonds, can be observed from Raman spectra. Similar results can also be found from FTIR spectra.

Furthermore, ^{13}C, ^{11}B, and ^{7}Li solid-state NMR spectra show more detailed differences between $(LiBH_4)_2$·en, LiBH4·en, and the starting materials (Figures S2−S4, Supporting Information). Since en is liquid at RT, the ^{13}C NMR spectrum of en was carried out without rotation. The peak at 45.6 ppm corresponding to N−C−C−N was observed in en. Broad peaks ranging from 43.0 to 48.0 ppm and 44.0 to 49.0 ppm were detected in $(LiBH_4)_2$·en and $LiBH_4$·en, respectively, which can be attributed to the retention of N−C−C−N bonds. Figure S3 (Supporting Information) shows the ^{11}B NMR spectra of $(LiBH_4)_2$·en, $LiBH_4$·en, and $LiBH_4$. The chemical shift at −41.9 ppm was found in $LiBH_4$. In the spectra of $(LiBH_4)_2$·en and $LiBH_4$·en, the signals of ^{11}B shifted to −41.2 and −41.8 ppm, respectively. In ^{7}Li NMR spectra, the chemical shift of ^{7}Li in $(LiBH_4)_2$·en was found at 0.01 ppm, which is much different from those in $LiBH_4$·en (δ = 0.27 ppm) and $LiBH_4$ (δ = 0.28 ppm). The shifts of ^{11}B and ^{7}Li in $(LiBH_4)_2$·en and $LiBH_4$·en may be caused by the changes of B and Li chemical environments.

Structure Determination. The crystal structures of the three kinds of N containing ligand complexes, including $LiBH_4$−NH_3, $LiBH_4$−NH_2NH_2, and $LiBH_4$−en complexes, are summarized in Table 1. The crystal structure of $LiBH_4$·NH_3 with the lattice parameters of a = 5.07213(2) Å, b = 4.46432(1) Å, c = 14.34875(0) Å, and V = 382.6 Å^3 was reported by Johnson et al. and Guo et al., separately.[32,39] More recently, studied by He et al., the XRD patterns of $(LiBH_4)_2$·N_2H_4 and $LiBH_4$·N_2H_4 were indexed using an orthorhombic $P2_12_12_1$ cell and a monoclinic Cc cell with lattice parameters of a = 7.6930(6) Å, b = 11.913(1) Å, c = 7.4985(1) Å, V = 631.95(15) Å^3 and a = 12.0638 Å, b = 5.7217 Å, c = 10.3680 Å, β = 104.75°, V = 821.08 Å^3, respectively.[31,40]

In this work, XRD patterns and the Rietveld fits of newly synthesized $(LiBH_4)_2$·en and $LiBH_4$·en are shown in Figure 2. XRD patterns of the samples do not contain any detectable phases of $LiBH_4$ showing quantitative conversion of the starting chemicals. The new sets of diffraction peaks emerged in $(LiBH_4)_2$·en and $LiBH_4$·en samples can be well matched by a monoclinic $P2_1/c$ and a monoclinic Pn cell, with lattice parameters of a = 17.1333(18) Å, b = 4.5202(4) Å, c = 11.4634(10) Å, β = 106.158(5)° and a = 8.2428(22) Å, b = 5.2363(4) Å, c = 8.2364(11) Å, β = 116.110(3)°, respectively.

On the basis of powder XRD data, crystal structures of $(LiBH_4)_2$·en and $LiBH_4$·en were determined by performing combined direct space simulated annealing and first-principle calculations. It is worth highlighting that a rare bridging coordination mode of en is observed in $(LiBH_4)_2$·en and $LiBH_4$·en. Up to date, coordination compounds containing bridging en units are relatively less studied, although a few extended structures (chains, sheets, and 3D networks) are reported.[42−44] In $(LiBH_4)_2$·en and $LiBH_4$·en, the en molecules are equivalent, each of which links with two Li^+ centers by the interaction between Li^+ and the [NH_2] groups at two ends of en (Figure S11A, Supporting Information). In $LiBH_4$·en, [Li^+−en−Li^+−BH_4^-] chains form a special double helix structure

dx.doi.org/10.1021/jp503123d | J. Phys. Chem. C 2014, 118, 13451−13459

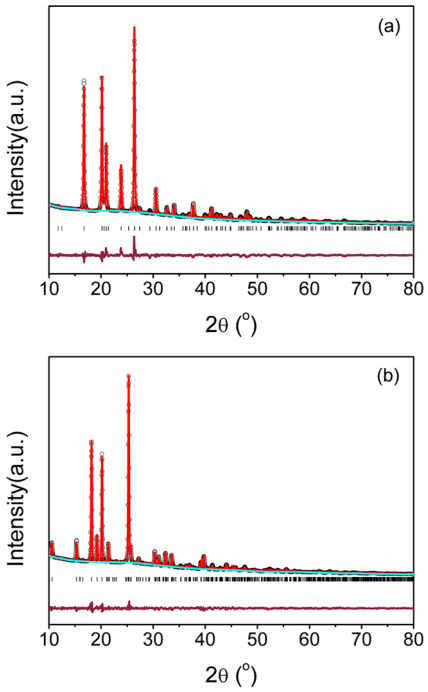

Figure 2. Experimental (circles), fitted (line), and difference (line below observed and calculated patterns) XRD profiles of (a) $LiBH_4$·en and (b) $(LiBH_4)_2$·en at 298 K (Cu Kα radiation). Vertical bars indicate the calculated positions of Bragg peaks.

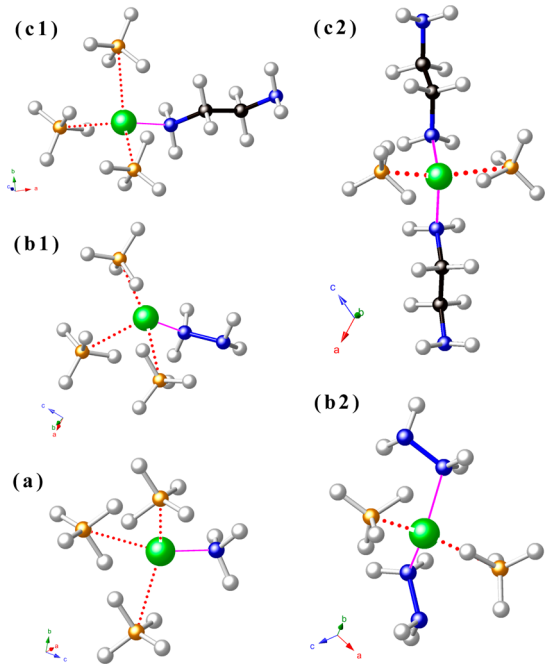

Figure 3. Close contacts around the Li center in (a) $LiBH_4$·NH_3, (b1) $(LiBH_4)_2$·N_2H_4, (b2) $LiBH_4$·N_2H_4, (c1) $(LiBH_4)_2$·en, and (c2) $LiBH_4$·en. Li cations are indicated as green spheres, while B, N, H, and C atoms are orange, blue, white, and black spheres, respectively.

(Figure S11B, Supporting Information). In addition, alternating the Li^+ center and $[BH_4^-]$ in $LiBH_4$·en forms infinite $[(Li^+)(BH_4^-)]$ chains (Figure S11C, Supporting Information). The structure of $LiBH_4$·en shows a 3D network that consists of $[LiN_2(BH_4)_2]$ tetrahedrons linked by en molecules and $[BH_4^-]$ groups (Figure S11D, Supporting Information). In $(LiBH_4)_2$·en, the structure of $(LiBH_4)_2$·en contains 2D sheets along the *b* axis (Figure S11E, Supporting Information). In addition to the bridging of en to form a $[Li^+$—en—$Li^+]$ chain, the chains are interconnected by two $[BH_4^-]$ via head-to-head or tail-to-tail coordination, forming four-membered rings of $[(Li^+)_2(BH_4^-)_2]$ at each edge (Figure S11F, Supporting Information).

As shown in Figure 3, tetrahedral coordination of lithium ions is observed in $(LiBH_4)_2$·en and $LiBH_4$·en. Compared with $LiBH_4$—NH_3 and $LiBH_4$—N_2H_4 complexes, it is interesting that these $LiBH_4$—N containing ligand complexes have the same Li/N molar ratio showing similar coordination environments. For example, at the Li/N ratio of 1 to 1 in $(LiBH_4)_2$·en, $(LiBH_4)_2$·N_2H_4, and $LiBH_4$·NH_3 complexes, the tetrahedral coordination of the Li cation by three $[BH_4^-]$ ions and one $[NH_2]$ group (or NH_3) was clearly observed. At a Li/N ratio of 1 to 2, Li atoms are tetrahedrally surrounded by two $[BH_4^-]$ units and two $[NH_2]$ groups, as depicted in $LiBH_4$·en and $LiBH_4$·N_2H_4 (Figure 3b2 and c2). Interestingly, increasing the Li/N ratio to 1/4, as shown in $LiBH_4$·2en and $LiBH_4$·$2N_2H_4$, resulted in tetracoordination of the $[NH_2]$ group to the Li cation.[31,41] Thus, it is clearly illustrated that the Li center tends to be surrounded by more $[NH_2]$ groups with the increasing number of N containing ligands.

The changes of coordination environments may also affect the bond distances in these complexes. Their main distances have been summarized in Table 2. The Li—B and Li—N distances in $(LiBH_4)_2$·en are in the range of 2.396—2.741 Å and 2.063—2.064 Å, respectively. However, the Li—B and Li—N distances are in the range of 2.40(2)—2.50(6) Å and 2.11(0)—2.20(1) Å in $LiBH_4$·en. All $LiBH_4$—N containing ligand complexes contain $H^{\delta+}$ (in the $[NH_2]$ group) and $H^{\delta-}$ (in $[BH_4^-]$) in the molecules. The interactions between the oppositely charged hydrogen atoms result in the elongated N—H and B—H distances compared to those in the pristine $LiBH_4$[45] and amines,[46,47] which lead to the red shifts of N—H and B—H vibrations in Raman and FTIR spectra. The shortest distances of BH···HN are all less than 2.4 Å in the above-mentioned complexes (Table 2), indicating the establishment of dihydrogen bonding in the structures. The dihydrogen bonding in ammonia borane is considered as primarily responsible for the stability of this molecular crystal at RT.[48] Similarly, structures of $LiBH_4$—N containing ligand complexes are stabilized by the strong dihydrogen bonding between N containing ligands and $[BH_4^-]$ as well as by the interactions between Li^+ and N containing ligands throughout the crystal structures. These interactions are expected to have profound impacts on their thermal behaviors.

Thermal Behaviors in Open Systems. Thermal behaviors of $(LiBH_4)_2$·en and $LiBH_4$·en were first investigated in open systems by TG-DTA and TPD-MS under Ar flow. As shown in the DTA curves (Figure 4), it is worth noting that endothermic reactions at 100 and 93 °C were observed in $(LiBH_4)_2$·en and $LiBH_4$·en during the heating process at a ramping rate of 1 °C min^{-1}, respectively. These reactions were found to be exothermic and shifted to lower temperatures (88 and 74 °C) when cooled from 130 °C at 0.2 °C min^{-1}. The reversible transformations during the heating and cooling processes without any detectable weight losses (Figure 5) indicate the melting nature of $(LiBH_4)_2$·en and $LiBH_4$·en. The hysteresis between melting and solidification curves is a common phenomenon, which may be caused by the differences in heating and cooling rates or the undercooling nature of the complexes.

dx.doi.org/10.1021/jp503123d | J. Phys. Chem. C 2014, 118, 13451—13459

Table 2. Interatomic Distances (Å) in $(LiBH_4)_2$·en and $LiBH_4$·en Compared with $LiBH_4$·NH_3, $(LiBH_4)_2$·N_2H_4, and $LiBH_4$·N_2H_4 at Room Temperature

	$(LiBH_4)_2$·en	$LiBH_4$·en	$(LiBH_4)_2$·N_2H_4	$LiBH_4$·N_2H_4	$LiBH_4$·NH_3
B···H	1.22(4)−1.24(4)	1.22(5)−1.22(9)	1.22(4)−1.22(6)	1.21(7)−1.23(1)	1.21(7)−1.24(0)
N···H	1.03(2)	1.02(5)−1.02(7)	1.03(0)−1.03(1)	1.02(5)−1.03(6)	1.03(4)−1.08(8)
C···N	1.47(6)	1.46(7)−1.47(1)	-	-	-
Li···B	2.39(6)−2.74(1)	2.40(2)−2.50(6)	2.35(8)−2.71(8)	2.32(2)−2.60(0)	2.50(7)−2.58(2)
Li···N	2.06(3)−2.06(4)	2.11(0)−2.20(1)	2.13(2)−2.13(3)	2.13(1)−2.42(7)	1.89(4)
shortest BH···HN	1.94(9)	2.06(7)	1.87(8)	2.06(6)	2.25(4)

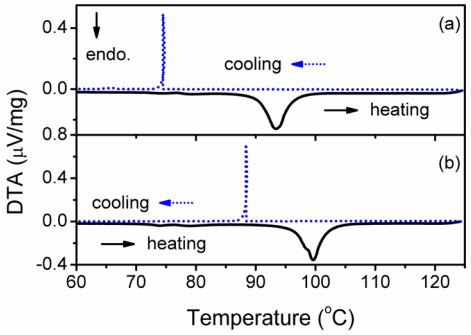

Figure 4. DTA curves of (a) $LiBH_4$·en and (b) $(LiBH_4)_2$·en during heating and cooling processes.

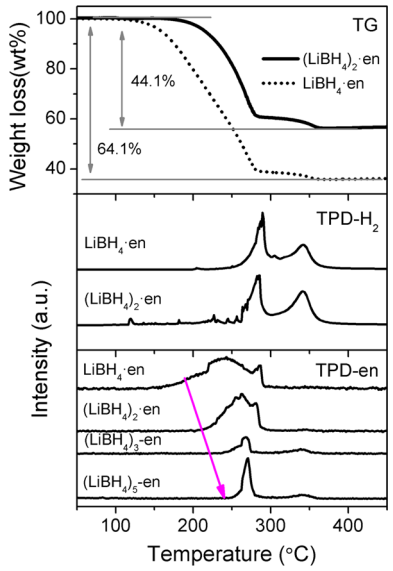

Figure 5. TG and TPD-MS results of $LiBH_4$−en complexes.

From TG and TPD-MS results in Figure 5, it can be seen that $(LiBH_4)_2$·en and $LiBH_4$·en start to decompose at temperatures above 180 and 150 °C, respectively. The decompositions of $(LiBH_4)_2$·en and $LiBH_4$·en include detachment of en ligands and dehydrogenation. As shown in the TPD-MS results, en molecules were desorbed from $(LiBH_4)_2$·en and $LiBH_4$·en in the temperature ranges of 180−290 °C and 150−290 °C, respectively. Dehydrogenations of both complexes in the second step occur in the temperature range of 250−380 °C. From TG measurements, the total mass losses observed from $(LiBH_4)_2$·en and $LiBH_4$·en were 44.1 and 64.1 wt %, respectively. The first steps in TG curves were mainly involved in the detachment of en, which is about 0.65 and 0.8 equiv of en from $(LiBH_4)_2$·en and $LiBH_4$·en, respectively. The same intermediates of a mixture of $(LiBH_4)_2$·en and $LiBH_4$ were observed in $(LiBH_4)_2$·en and $LiBH_4$·en after heating to 250 °C as shown in Figure S12 (Supporting Information). Then, the intermediates in both $(LiBH_4)_2$·en and $LiBH_4$·en may decompose in the same way when heating to higher temperatures. The possible decomposition pathways of $(LiBH_4)_2$·en and $LiBH_4$·en can be described in Scheme 1. There are three steps for decomposition of $LiBH_4$ ethylenediaminates: (1) detachment of en molecules with formation of $(LiBH_4)_2$·en and $LiBH_4$; (2) dehydrogenation of $(LiBH_4)_2$·en with formation of $[LiBH_4]$ and $Li[BN_2C_2H_4]$, here $[LiBH_4]$, may complex with other species, and $Li[BN_2C_2H_4]$ only shows the contents of each element in the products; (3) decomposition of $LiBH_4$ and $[LiBH_4]$. The total weight losses from $(LiBH_4)_2$·en and $LiBH_4$·en calculated from Scheme 1 are approximately 44.95 and 63.38 wt %, which agree well with the TG results.

It is well understood that coordination strength is a matter of the number of ligands coordinated with the metal center which has been found in the halide−ammonia complexes.[49−51] The desorption of ammonia from $Ca(NH_3)_8Cl_2$, $Mn(NH_3)_6Cl_2$, $Mg(NH_3)_6Cl_2$, and $Ni(NH_3)_6Cl_2$ examined by TG-MS was found to be a multistep reaction.[49] That is to say, the more NH_3 coordinates with a metal center, the easier it would be detached. Similar results have been observed in $LiBH_4$−N_2H_4 complexes.[40] $(LiBH_4)_2$·N_2H_4 evolves hydrazine at around 220

Scheme 1. Possible Decomposition Pathways of $(LiBH_4)_2$·en and $LiBH_4$·en

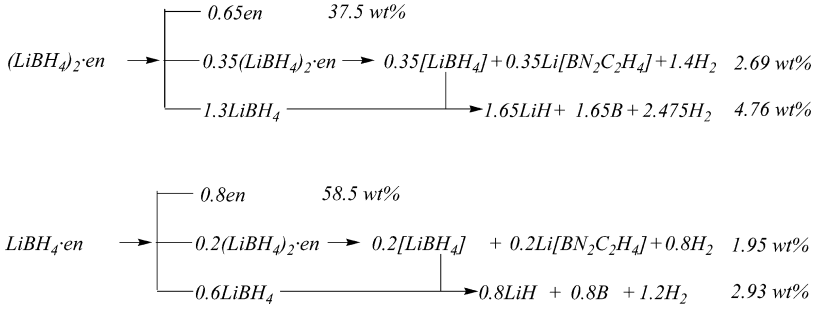

dx.doi.org/10.1021/jp503123d | J. Phys. Chem. C 2014, 118, 13451−13459

°C which is higher than that of $LiBH_4{\cdot}N_2H_4$ (165 °C). $(LiBH_4)_3{\cdot}N_2H_4$ does not release any detectable hydrazine in the temperature range of 20−500 °C. To find the coordination strength of $LiBH_4$ and en, two additional samples of $(LiBH_4)_3$−en and $(LiBH_4)_5$−en were prepared by ball milling. However, only $(LiBH_4)_2{\cdot}$en and $LiBH_4$ phases were observed in both samples, as evidenced by XRD (Figure S5, Supporting Information). As shown in Figure 5, en desorption temperatures of $LiBH_4{\cdot}$en, $(LiBH_4)_2{\cdot}$en, $(LiBH_4)_3$−en, and $(LiBH_4)_5$−en are 150, 180, 230, and 250 °C, respectively. These results are in accordance with those observed in $LiBH_4{-}N_2H_4$ complexes in which the coordination strength between Li^+ and the ligands decreases with the increasing number of en. Although the structure parameters cannot provide a direct explanation for the above phenomena since the samples have melted before decomposition, the studies of Li−N distances in the complexes can also give us some inspiration. As shown in Table 2, Li−N distances in $LiBH_4$−N containing ligand complexes are elongated with the increase of ligands, meaning the weakening of Li^+/ligand interaction.

It was reported that the establishment of NH···HB dihydrogen bonding networks plays a significant role in promoting dehydrogenation of ammonia borane.[48] For $LiBH_4$−en complexes, hydrogen is first released from $(LiBH_4)_2{\cdot}$en in open systems. Similarly, dehydrogenation of $LiBH_4{\cdot}NH_3$ and $(LiBH_4)_2{\cdot}N_2H_4$ has been reported.[31,39] As shown in Table 2, the shortest NH···HB distances in $LiBH_4{\cdot}NH_3$, $(LiBH_4)_2{\cdot}$en, and $(LiBH_4)_2{\cdot}N_2H_4$ are 2.25(4), 1.94(9), and 1.87(8) Å, respectively. Accordingly, the dehydrogenation temperatures are about 280, 260, and 235 °C for $LiBH_4{\cdot}NH_3$, $(LiBH_4)_2{\cdot}$en, and $(LiBH_4)_2{\cdot}N_2H_4$, respectively. Similar to the dehydrogenation of NH_3BH_3, hydrogen gas may be released from $LiBH_4$−N containing ligand complexes through the combination of $H^{\delta+}$ in ligands and $H^{\delta-}$ in $[BH_4^-]$. Therefore, the shortest NH···HB distance gives rise to the strongest $H^{\delta+}\cdots H^{\delta-}$ interaction and results in the lowest dehydrogenation temperature of $LiBH_4$−N containing ligand complexes. The relationship between NH···HB distances and dehydrogenation temperature has been verified from a meager energy barrier to dehydrogenation in the previous report.[52] The shortest NH···HB distance in the transition state for dehydrogenation is ~0.988 Å. The barrier for dehydrogenation seems to be proportional to the NH···HB distances in the $LiBH_4$−N containing ligand complexes. The large distance reorganization from complexes with longer NH···HB bonds to the transition state is expected to require more energy than in the cases of complexes with shorter NH···HB bonds. Therefore, hydrogen can be released at lower temperatures from the complexes with shorter NH···HB distances.

Catalytic Dehydrogenation in a Closed System. Quantitative measurements on hydrogen desorption from the samples were subsequently investigated using a Sievert-type apparatus. Approximately 200 mg samples were loaded into a closed vessel with a heating rate of 2 °C min^{-1} each time. The pressure increase in the vessel was monitored by a digital pressure gauge. The amount of gaseous products can be calculated by use of the ideal gas equation ($PV = nRT$). After that, small amounts of gaseous products will be connected from the pressurized vessel to MS for analysis. As shown in Figure 6A, both the pristine $(LiBH_4)_2{\cdot}$en and $LiBH_4{\cdot}$en decompose slowly at 180 °C, evolving 0.89 and 0.78 equiv of gases per en after heating for 12 h. Interestingly, hydrogen is the only detectable gaseous product as shown in Figure 6B. In the cases

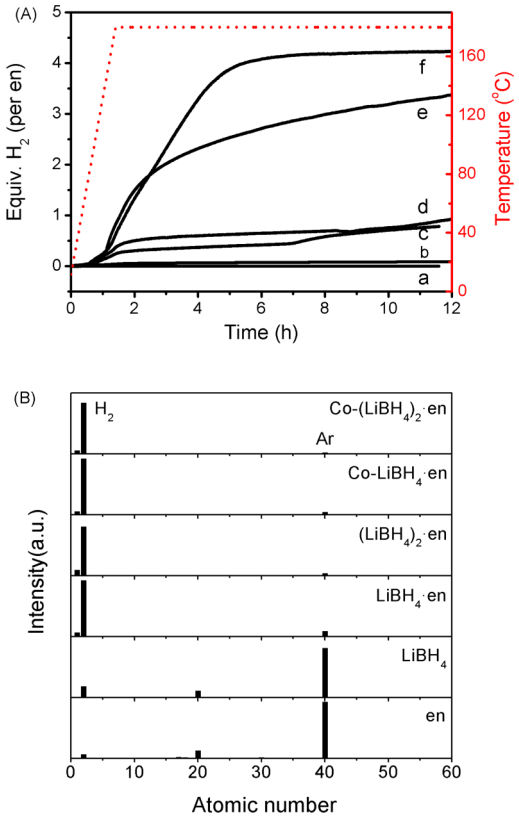

Figure 6. (A) Volumetric release measurements on (a) en, (b) $LiBH_4$, (c) pristine $LiBH_4{\cdot}$en, (d) pristine $(LiBH_4)_2{\cdot}$en, (e) Co-doped $LiBH_4{\cdot}$en, and (f) Co-doped $(LiBH_4)_2{\cdot}$en at 180 °C. (B) MS profiles of the gaseous products of en, $LiBH_4$, $LiBH_4{\cdot}$en, $(LiBH_4)_2{\cdot}$en, Co-doped $LiBH_4{\cdot}$en, and Co-doped $(LiBH_4)_2{\cdot}$en after heating for 12 h at 180 °C. Hydrogen was the only detectable gaseous product. The detected Ar was from the glovebox where the sample was loaded into the vessel.

of $LiBH_4{-}NH_3$ and $LiBH_4{-}N_2H_4$ complexes, NH_3 and NH_3/N_2 are the main byproducts during the dehydrogenation. Due to the strong C−N bonds, neither NH_3 nor N_2 was found in the dehydrogenation products of $LiBH_4$−en complexes. It was reported by Zheng et al. that the thermal decomposition pathway of $LiBH_4{\cdot}NH_3$ can be altered by "locking" NH_3 in the vicinity of $LiBH_4$ to increase the chance of dehydrogenation rather than deammonization.[53] The way to retain NH_3 in the materials is through equilibrium−vapor−pressure, i.e., by putting the ammoniate in a closed vessel, which is similar to the volumetric release experiment performed in this study. Therefore, direct dehydrogenation took place rather than desorption of en from $(LiBH_4)_2{\cdot}$en and $LiBH_4{\cdot}$en due to the retainment of en in the vicinity of $LiBH_4$ in such a closed system. However, the pristine samples show poor dehydrogenation kinetics at 180 °C, and only 22.2% and 19.2% of the ideal dehydrogenation amounts of $(LiBH_4)_2{\cdot}$en and $LiBH_4{\cdot}$en can be achieved after heating for 12 h, respectively.

Previous investigations on $LiBH_4{-}NH_3$ and $LiBH_4{-}N_2H_4$ complexes revealed that transition metals, such as Co and Fe, can be effective catalysts in promoting dehydrogenation, especially when the sample is in the melting state. This is understandable since the molten sample will be mobile and has higher chances to interact with catalyst.[54] As mentioned above, $(LiBH_4)_2{\cdot}$en and $LiBH_4{\cdot}$en melt at 100 and 93 °C, respectively. Therefore, the $CoCl_2$ precursor was introduced into $(LiBH_4)_2{\cdot}$en and $LiBH_4{\cdot}$en by ball milling. Volumetric release experi-

dx.doi.org/10.1021/jp503123d | J. Phys. Chem. C 2014, 118, 13451−13459

ments show that ca. 3.5 and 4.0 equiv of H_2 per en evolved from the Co-catalyzed $LiBH_4$·en and $(LiBH_4)_2$·en at 180 °C as shown in Figure 6A (e, f), respectively, showing the rapid interaction between en and $LiBH_4$ during the heating process in the presence of Co-based catalyst. In other words, around 8.5 and 7.7 wt % of hydrogen can be released from Co-catalyzed $LiBH_4$·en and $(LiBH_4)_2$·en, respectively. At the same condition, only 1.9 and 1.7 wt % of H_2 can evolve from $LiBH_4$·en and $(LiBH_4)_2$·en, and the starting materials, $LiBH_4$ and en, release only negligible gases product. The evolution of H_2 gas from Co-doped $LiBH_4$·en and $(LiBH_4)_2$·en was verified by MS measurements as shown in Figure 6B. As shown by previous reports in the literature, chemical states of Co catalyst in $LiBH_4$–NH_3 and $LiBH_4$–$LiNH_2$ complexes may be Co or CoB alloy.[54] It is most likely that the reduced Co is produced by the reaction of $CoCl_2$ precursor and $[BH_4^-]$.[53] Therefore, Co or CoB alloy may also be the active species in Co-catalyzed $LiBH_4$·en and $(LiBH_4)_2$·en.

The solid dehydrogenated products were characterized by XRD and solid-state ^{11}B MAS and ^{13}C CPMAS NMR. As shown in Figure S6 (Supporting Information), several weak peaks were observed at 7.4°, 19.8°, 24.0°, etc. in the XRD patterns of the dehydrogenated residues of $(LiBH_4)_2$·en and $LiBH_4$·en. However, these peaks cannot match with any known species from the database. In ^{13}C CPMAS NMR spectra, the dehydrogenated residues present two peaks at 47.2 and 51.2 ppm (Figure S7, Supporting Information), indicating that C still keeps the sp^3-hybridized state and bonds with H, C, and N.[55,56] Therefore, N–C–C–N bonds are retained in the products. ^{11}B MAS NMR spectra of the residues exhibit a broad line shape with two overlapped peaks at 28.0 and 23.0 ppm (Figure S8, Supporting Information), revealing the existence of sp^2-hybridized B species in the BN_2H or BN_3 environment. Similar ^{11}B MAS NMR spectra have been observed in the study of hexagonal BN, BNH_x, and [LiNBH].[57] ^{11}B signals at −40 ppm, which are the signals of $[BH_4^-]$, were found in both samples. Obviously, the $[BH_4^-]$ signal in dehydrogenated $LiBH_4$·en residues is much weaker than that in $(LiBH_4)_2$·en. There are equivalent $H^{\delta+}$ and $H^{\delta-}$ in $LiBH_4$·en, while, $H^{\delta-}$ in $(LiBH_4)_2$·en is two times more than $H^{\delta+}$. It is believable that 4 equiv of H_2 may be released from both $LiBH_4$·en and $(LiBH_4)_2$·en due to the interaction between $H^{\delta+}$ and $H^{\delta-}$. In $LiBH_4$·en, $H^{\delta+}$ in en and $H^{\delta-}$ in $[BH_4^-]$ will be totally consumed. However, in $(LiBH_4)_2$·en, $H^{\delta+}$ in en will be completely consumed, and the excess $H^{\delta-}$ in $[BH_4^-]$ will remain. Therefore, the $[BH_4^-]$ signals in NMR spectra can probably be ascribed to a minor unreacted $LiBH_4$·en in the dehydrogenated $LiBH_4$·en and remaining $[BH_4^-]$ groups in dehydrogenated $(LiBH_4)_2$·en, respectively. Thus, the dehydrogenated residues of $(LiBH_4)_2$·en may be comprised of Li^+, $[BH_4^-]$, and $[-B{=}NCH_2CH_2N-]_n^{n-}$. On the other hand, totally dehydrogenated residues of $LiBH_4$·en only contain species composed of Li^+ and $[-B{=}NCH_2CH_2N-]_n^{n-}$. Nevertheless, the actual compositions and structures of $[-B{=}NCH_2CH_2N-]_n^{n-}$ remain uncertain, and further investigation is needed to clarify the dehydrogenation products in the future.

CONCLUSIONS

The coordination of en to the Li center of borohydrides leads to the formation of lithium borohydride ethylenediaminates. By comparison of $LiBH_4$–NH_3, $LiBH_4$–N_2H_4, and $LiBH_4$–en complexes, similar coordination environments of Li^+ were observed in the complexes having the same Li/N molar ratios. When heated in an open system, lithium borohydride ethylenediaminates decomposed via detachment of en followed by dehydrogenation. Three-step pathways including releasing of en, dehydrogenation of $(LiBH_4)_2$·en, as well as the decomposition of $LiBH_4$ and remaining $[BH_4^-]$ were proposed. With the decreasing number of en, en detaching temperatures increased from 150 to 250 °C. The onset dehydrogenation temperatures were related to the shortest NH···HB distances in the $LiBH_4$–N containing ligand complexes. The shortest NH···HB distance gives rise to the strongest $H^{\delta+}\cdots H^{\delta-}$ interaction, which results in the lowest dehydrogenation temperature of $LiBH_4$–N containing ligand complexes. When heated in a closed system, direct dehydrogenation without release of ligands can be achieved at relatively low temperatures by loading the complexes into a closed vessel with Co-based catalyst. About 8.5 and 7.7 wt % of hydrogen can be released from Co-catalyzed $LiBH_4$·en and $(LiBH_4)_2$·en at 180 °C, respectively. The above results may be a guideline for the study of other $LiBH_4$–organic amine complexes, which may find potential applications in organic synthesis, catalysis, Li ion conductivity, and hydrogen generation.

ASSOCIATED CONTENT

Supporting Information

A description of calculation methods on lithium borohydride ethylenediaminates, tables of $LiBH_4$ coordination compound with ethers and amines, TPD-MS results of $LiBH_4$·2en, figures of ^{13}C, ^{11}B, and ^7Li NMR spectra of $(LiBH_4)_2$·en, $LiBH_4$·en, neat $LiBH_4$, and neat en, figure of XRD patterns of $(LiBH_4)_n$·en and $LiBH_4$, figure of XRD patterns of Co-doped $(LiBH_4)_2$·en and $LiBH_4$·en after dehydrogenation, figures of ^{13}C and ^{11}B NMR spectra of $LiBH_4$·en and $(LiBH_4)_2$·en before and after dehydrogenation, photos of the as-prepared samples, photos of the sample exposure to air, crystal structures of $(LiBH_4)_2$·en and $LiBH_4$·en, and XRD patterns of the decomposition products of $(LiBH_4)_2$·en and $LiBH_4$·en collected at different temperatures. This material is available free of charge via the Internet at http://pubs.acs.org.

AUTHOR INFORMATION

Corresponding Authors

*E-mail: pchen@dicp.ac.cn. Tel./Fax: +86 411 84379583.
*E-mail: wgt@dicp.ac.cn.

Notes

The authors declare no competing financial interest.

ACKNOWLEDGMENTS

The authors would like to acknowledge the Project of National Natural Science Funds for Distinguished Yong Scholar (51225206), 973 (2010CB631304) Project, National Natural Science Foundation of China (U1232120, 51301161), Postdoctoral Science Foundation Funded Project, and Shanghai Synchrotron Radiation Facility (SSRF) for providing the beam time.

REFERENCES

(1) Zeynizadeh, B.; Behyar, T. Wet THF as a Suitable Solvent for a Mild and Convenient Reduction of Carbonyl Compounds with $NaBH_4$. *Bull. Chem. Soc. Jpn.* **2005**, *78*, 307–315.
(2) Larock, R. C. *Comprehensive Organic Transformations: A Guide to Functional Group Preparations*; Wiley-VCH: New York, 1999.
(3) Hudlicky, M. *Reductions in Organic Chemistry*; American Chemical Society: Washington, DC, 1996.

(4) Barone, V.; Dolcetti, G.; Lelj, F.; Russo, N. Transition-Metal Tetrahydroborate Complexes as Catalysts. 1. Nonempirical Determination of Static, Dynamic, and Chemical Properties of the Model Compounds Sodium Tetrahydroborate and Aluminum Borate (AlH_2BH_4). *Inorg. Chem.* **1981**, *20*, 1687−1691.
(5) Chaikin, S. W.; Brown, W. G. Reduction of Aldehydes, Ketones and Acid Chlorides by Sodium Borohydride. *J. Am. Chem. Soc.* **1949**, *71*, 122−125.
(6) Reyes-Márquez, V.; Lara, K. O.; Sánchez, M.; Gálvez-Ruizb, J. C. Unconventional Hydrogen and Dihydrogen Bonded Supramolecular Array of a 2,6-Dioxa-9,16-Diaza-1,3(1,2),4(1,4)-Tribenzenacycloheptadecaphane-Borane Adduct. *Arkivoc* **2008**, *115*, 123.
(7) Makhaev, V. D. Structural and Dynamic Features of Tetrahydroborate Complexes. *Usp. Khimii.* **2000**, *69*, 795−816.
(8) Moussa, G.; Moury, R.; Demirci, U. B.; Sener, T.; Miele, P. Boron-Based Hydrides for Chemical Hydrogen Storage. *Int. J. Energy Res.* **2013**, *37*, 825−842.
(9) Vajo, J. J.; Skeith, S. L.; Mertens, F. Reversible Storage of Hydrogen in Destabilized $LiBH_4$. *J. Phys. Chem. B* **2005**, *109*, 3719−3722.
(10) Züttel, A.; Wenger, P.; Rentsch, S.; Sudan, P.; Mauron, P.; Emmenegger, C. $LiBH_4$ a New Hydrogen Storage Material. *J. Power Sources* **2003**, *118*, 1−7.
(11) El Kharbachi, A.; Pinatel, E.; Nuta, I.; Baricco, M. A Thermodynamic Assessment of $LiBH_4$. *Calphad* **2012**, *39*, 80−90.
(12) Schlesinger, H. I.; Brown, H. C. Metallo Borohydrides. III. Lithium Borohydride. *J. Am. Chem. Soc.* **1940**, *62*, 3429−3435.
(13) Harris, P. M.; Meibohm, E. P. The Crystal Structure of Lithium Borohydride $LiBH_4$. *J. Am. Chem. Soc.* **1947**, *69*, 1231−1232.
(14) Pistorius, C. W. Melting and Polymorphism of $LiBH_4$ to 45 kbar. *Z. Phys. Chem.* **1974**, *88*, 253−263.
(15) Fedneva, E.; Alpatova, V.; Mikheeva, V. $LiBH_4$ Complex Hydride Materials. *Russ. J. Inorg. Chem.* **1964**, *9*, 826−7.
(16) Soloveichik, G. L.; Andrus, M.; Gao, Y.; Zhao, J. C.; Kniajanski, S. Magnesium Borohydride as a Hydrogen Storage Material: Synthesis of Unsolvated $Mg(BH_4)_2$. *Int. J. Hydrogen Energy* **2009**, *34*, 2144−2152.
(17) Ephritikhine, M. Synthesis, Structure, and Reactions of Hydride, Borohydride, and Aluminohydride Compounds of the F-Elements. *Chem. Rev.* **1997**, *97*, 2193−2242.
(18) Klingen, T. J. Reaction of Copper (II) Chloride with Lithium Borohydride. *Inorg. Chem.* **1964**, *3*, 1058−1059.
(19) Goudon, J. P.; Bernard, F.; Renouard, J.; Yvart, P. Experimental Investigation on Lithium Borohydride Hydrolysis. *Int. J. Hydrogen Energy* **2010**, *35*, 11071−11076.
(20) Takahashi, K.; Hattori, K.; Yamazaki, T.; Takada, K.; Matsuo, M.; Orimo, S.; Maekawa, H.; Takamura, H. All-Solid-State Lithium Battery with $LiBH_4$ Solid Electrolyte. *J. Power Sources* **2013**, *226*, 61−64.
(21) Sveinbjörnsson, D.; Myrdal, J. S. G.; Blanchard, D.; Bentzen, J. J.; Hirata, T.; Mogensen, M. B.; Norby, P.; Orimo, S.-I.; Vegge, T. Effect of Heat Treatment on the Lithium Ion Conduction of the $LiBH_4$−LiI Solid Solution. *J. Phys. Chem. C* **2013**, *117*, 3249−3257.
(22) Matsuo, M.; Takamura, H.; Maekawa, H.; Li, H.-W.; Orimo, S.-i., Stabilization of Lithium Superionic Conduction Phase and Enhancement of Conductivity of $LiBH_4$ by LiCl Addition. *Appl. Phys. Lett.* **2009**, *94*, 084103.
(23) Matsuo, M.; et al. Complex Hydrides with $(BH_4)^-$ and $(NH_2)^-$ Anions as New Lithium Fast-Ion Conductors. *J. Am. Chem. Soc.* **2009**, *131*, 16389−16391.
(24) Matsuo, M.; Nakamori, Y.; Orimo, S.-i.; Maekawa, H.; Takamura, H. Lithium Superionic Conduction in Lithium Borohydride Accompanied by Structural Transition. *Appl. Phys. Lett.* **2007**, *91*, 224103.
(25) Aguilar-Martínez, M.; Félix-Baéz, G.; Pérez-Martínez, C.; Nöth, H.; Flores-Parra, A.; Colorado, R.; Galvez-Ruiz, J. C. Studies in Solution and the Solid State of Coordination Compounds Derived from $LiBH_4$, $NaBH_4$, and Bidentate Aromatic Amines. *Eur. J. Inorg. Chem.* **2010**, *2010*, 1973−1982.
(26) Galvez-Ruiz, J. C.; Sanchez, M. Structural Analysis of Alkali Metal Tetrahydroborates: The Role of Metal and Coordination Form in the $[BH_4]^-$ Anion Structure. *J. Mol. Struct.: THEOCHEM* **2009**, *908*, 114−116.
(27) Gálvez Ruiz, J. C.; Nöth, H.; Warchhold, M. Coordination Compounds of Alkali Metal Tetrahydroborates with Ethers and Amines. *Eur. J. Inorg. Chem.* **2008**, *2008*, 251−266.
(28) Buttery, J. H. N.; Plackett, N. C.; Skelton, B. W.; Whitaker, C. R.; White, A. H. Syntheses and Structures of Lithium and Sodium Salt Complexes with Alkylpolyamine Ligands. *Z. Anorg. Allg. Chem.* **2006**, *632*, 1856−1869.
(29) Liu, L.; Hu, D.; He, T.; Zhang, Y.; Wu, G.; Chu, H.; Wang, P.; Xiong, Z.; Chen, P. Lithium Borohydride−Melamine Complex as a Promising Material for Chemical Hydrogen Storage. *J. Alloys Compd.* **2013**, *552*, 98−101.
(30) Sullivan, E. A.; Johnson, S. The Lithium Borohydride−Ammonia System P−C−T Relationships and Densities. *J. Phys. Chem.* **1959**, *63*, 233−238.
(31) He, T.; Wu, H.; Wu, G.; Wang, J.; Zhou, W.; Xiong, Z.; Chen, J.; Zhang, T.; Chen, P. Borohydride Hydrazinates: High Hydrogen Content Materials for Hydrogen Storage. *Energy Environ. Sci.* **2012**, *5*, 5686−5689.
(32) Johnson, S. R.; David, W. I. F.; Royse, D. M.; Sommariva, M.; Tang, C. Y.; Fabbiani, F. P. A.; Jones, M. O.; Edwards, P. P. The Monoammoniate of Lithium Borohydride, $Li(NH_3)BH_4$: An Effective Ammonia Storage Compound. *Chem.—Asian J.* **2009**, *4*, 849−854.
(33) Wu, H.; Zhou, W.; Pinkerton, F. E.; Meyer, M. S.; Srinivas, G.; Yildirim, T.; Udovic, T. J.; Rush, J. J. A New Family of Metal Borohydride Ammonia Borane Complexes: Synthesis, Structures, and Hydrogen Storage Properties. *J. Mater. Chem.* **2010**, *20*, 6550−6556.
(34) Guo, Y.; Gu, Q.; Guo, Z.; Mao, J.; Liu, H.; Dou, S.; Yu, X. A GBH/$LiBH_4$ Coordination System with Favorable Dehydrogenation. *J. Mater. Chem.* **2011**, *21*, 7138−7144.
(35) Armstrong, D. R.; Clegg, W.; Colquhoun, H. M.; Daniels, J. A.; Mulvey, R. E.; Stephenson, I. R.; Wade, K. Structure and Bonding of the Lithium Tetrahydroborate-Tetramethylethylenediamine Adduct $(TMEDA{\cdot}LiBH_4)_2$, a Centrosymmetric Dimer Containing Doubly and Triply Bridging Hydrogen Atoms. *J. Chem. Soc., Chem. Commun.* **1987**, 630−632.
(36) Giese, H.-H.; Habereder, T.; Nöth, H.; Ponikwar, W.; Thomas, S.; Warchhold, M. Metal Tetrahydridoborates and Tetrahydridoborato Metalates. 23.1 Amine Solvates of Lithium and Sodium Tetrahydridoborate. *Inorg. Chem.* **1999**, *38*, 4188−4196.
(37) Galvez-Ruiz, J. C.; Sanchez, M. Towards an Understanding of the Structure and Bonding of Lithium Tetrahydroborate and Its Amine Complexes. *J. Mol. Struct.: THEOCHEM* **2007**, *818*, 23−30.
(38) Lawrence, S. A. *Amines: Synthesis, Properties and Applications*; Cambridge University Press: New York, 2004.
(39) Guo, Y.; Xia, G.; Zhu, Y.; Gao, L.; Yu, X. Hydrogen Release from Amminelithium Borohydride, $LiBH_4{\cdot}NH_3$. *Chem. Commun.* **2010**, *46*, 2599−2601.
(40) He, T.; Wu, H.; Chen, J.; Zhou, W.; Wu, G.; Xiong, Z.; Zhang, T.; Chen, P. Alkali and Alkaline-Earth Metal Borohydride Hydrazinates: Synthesis, Structures and Dehydrogenation. *Phys. Chem. Chem. Phys.* **2013**, *15*, 10487−10493.
(41) Giese, Hans H.; Habereder, T.; Knizek, J.; Nöth, H.; Warchhold, M. Solvates of Lithium Tetrahydridoborates with Various Amines: From Molecular to Extended Structures of Lithium Tetrahydridoborate. *Eur. J. Inorg. Chem.* **2001**, *2001*, 1195−1205.
(42) Keene, T. D.; Hursthouse, M. B.; Price, D. J. Two-Dimensional Metal−Organic Frameworks: A System with Competing Chelating Ligands. *Cryst. Growth Des.* **2009**, *9*, 2604−2609.
(43) Huang, X.; Li, J.; Fu, H. The First Covalent Organic-Inorganic Networks of Hybrid Chalcogenides: Structures That May Lead to a New Type of Quantum Wells. *J. Am. Chem. Soc.* **2000**, *122*, 8789−8790.
(44) Rabenau, A.; Kniep, R.; Welzel, W. Phasengleichgewichte in Systemen Lithiumhalogenid-Ethylendiamin Sowie Die Kristallstruktu-

ren Von LiBr·($H_2NCH_2CH_2NH_2$), LiI·($H_2NCH_2CH_2NH_2$) Und LiI·3($H_2NCH_2CH_2NH_2$). *Z. Kristallogr.* **1988**, *183*, 179−191.
(45) Hartman, M. R.; Rush, J. J.; Udovic, T. J.; Bowman, R. C., Jr.; Hwang, S.-J. Structure and Vibrational Dynamics of Isotopically Labeled Lithium Borohydride Using Neutron Diffraction and Spectroscopy. *J. Solid State Chem.* **2007**, *180*, 1298−1305.
(46) Kohata, K.; Fukuyama, T.; Kuchitsu, K. Molecular Structure of Hydrazine as Studied by Gas Electron Diffraction. *J. Phys. Chem.* **1982**, *86*, 602−606.
(47) Lee, S. J.; Mhin, B. J.; Cho, S. J.; Lee, J. Y.; Kim, K. S. Ab Initio Studies of the Conformations of Methylamine and Ethylenediamine: Interaction Forces Affecting the Structural Stability. *J. Phys. Chem.* **1994**, *98*, 1129−1134.
(48) Staubitz, A.; Robertson, A. P. M.; Manners, I. Ammonia-Borane and Related Compounds as Dihydrogen Sources. *Chem. Rev.* **2010**, *110*, 4079−4124.
(49) Sørensen, R. Z.; Hummelshøj, J. S.; Klerke, A.; Reves, J. B.; Vegge, T.; Nørskov, J. K.; Christensen, C. H. Indirect, Reversible High-Density Hydrogen Storage in Compact Metal Ammine Salts. *J. Am. Chem. Soc.* **2008**, *130*, 8660−8668.
(50) Bevers, E.; van Ekeren, P.; Haije, W.; Oonk, H. Thermodynamic Properties of Lithium Chloride Ammonia Complexes for Application In a High-Lift High Temperature Chemical Heat Pump. *J. Therm. Anal. Calorim.* **2006**, *86*, 825−832.
(51) Christensen, C. H.; Sorensen, R. Z.; Johannessen, T.; Quaade, U. J.; Honkala, K.; Elmoe, T. D.; Kohler, R.; Norskov, J. K. Metal Ammine Complexes for Hydrogen Storage. *J. Mater. Chem.* **2005**, *15*, 4106−4108.
(52) Kulkarni, S. A. Intramolecular Dihydrogen Bonding in Main Group Elements. Connection with Dehydrogenation Reactions. *J. Phys. Chem. A* **1999**, *103*, 9330−9335.
(53) Zheng, X. L.; Wu, G. T.; Li, W.; Xiong, Z. T.; He, T.; Guo, J. P.; Chen, H.; Chen, P. Releasing 17.8 wt% H_2 from Lithium Borohydride Ammoniate. *Energy Environ. Sci.* **2011**, *4*, 3593−3600.
(54) Pinkerton, F. E.; Meisner, G. P.; Meyer, M. S.; Balogh, M. P.; Kundrat, M. D. Hydrogen Desorption Exceeding Ten Weight Percent from the New Quaternary Hydride $Li_3BN_2H_8$. *J. Phys. Chem. B* **2004**, *109*, 6−8.
(55) Tanaka, R.; Ueoka, I.; Takaki, Y.; Kataoka, K.; Saito, S. High Molecular Weight Linear Polyethylenimine and Poly(N-Methylethylenimine). *Macromolecules* **1983**, *16*, 849−853.
(56) Weyts, K.; Goethals, E. New Synthesis of Linear Polyethyleneimine. *Polym. Bull.* **1988**, *19*, 13−19.
(57) Gervais, C.; Maquet, J.; Babonneau, F.; Duriez, C.; Framery, E.; Vaultier, M.; Florian, P.; Massiot, D. Chemically Derived BN Ceramics: Extensive ^{11}B and ^{15}N Solid-State NMR Study of a Preceramic Polyborazilene. *Chem. Mater.* **2001**, *13*, 1700−1707.